The authors would like to thank the reviewers for their comments and feedback. Our answers are presented below in blue. For the minor comments, the check mark indicates that the suggested modification was implemented.

Major comments

Viewing Angle: Other studies have shown that microbolometer sensors suffer a significant reduction in measured temperatures when the viewing angle is greater than 40° (Cheng et al., 2012; Jiao et al., 2016; Litwa, 2010). This is potentially what is visible in Figure 5 of the manuscript at the periphery of the black body where viewing angle increases, though this could also be temperature bleeding across the boundary of the calibration surface and the background. When shooting thermal imagery from a nadir position (e.g. from a drone/plane) the viewing angle is generally less than 40° (unless flying over very complex topography) and this effect is minimised. However, when shooting an oblique as is the case in this manuscript much of the image is taken from angles exceeding 40°, when the land is sloping away (blue ellipses) from the camera this effect is enhanced, while when the land faces towards (red ellipses) the camera the effect is minimised. These errors are likely not picked up in the bias correction to the AWS stations because they all appear to have a very similar viewing angle from the camera. I would suggest first testing the sensor to see if, and to what extent it suffers from viewing angle errors (which is likely). If this is confirmed then these errors could be corrected by calculating the impact of viewing angle on their sensor in a lab using a black body of known temperature (as shown in Figure 5 of the manuscript) e.g. following Alexander & Lunderman, (2021) and then applying this correction to the image temperature measurements after calculating each pixels view angle from the camera.

According to our literature review, the variations of measured IR temperature due to the viewing angle depend on three possible elements:

1. the angular response of the sensors, the microbolometers. In this study the variation of the angular response is taken into account by the manufacturer's calibration of the instrument, and if this were not sufficient, the Flat Field Correction (FFC) would correct any potential residual angular response of the microbolometers.

2. vignetting, i. e. reduced luminosity in the periphery of the image due to the lens properties. This problem is also corrected by the FFC.

3. the directional emissivity of the target, as e.g. discussed in [Litwa(2010)]. As this issue was raised by both reviewers, the answer in the following paragraph is common to the two reviews.

As pointed out, the emissivity of snow is likely decreasing with the angle of observation. However, only few measurements of the directional snow emissivity are available in literature. These observations suggest that snow cover emissivity is mostly isotropic in contrast with most natural surfaces. However, angular variations were observed depending on several factors including density, age and grain size and there is no consensus on how to model them. To avoid an inappropriate correction, our approach is to consider that this effect contributes to the global error, that is assessed by the comparison with the ground truth measurements (that are not affected by the grazing incidence of the camera).

Nonetheless, to facilitate further investigation, as suggested by the reviewer, we add a map of the observation angles of the snow surface temperature in the published dataset.

To clarify this, the paragraph at L350 in the Discussion was modified as follows: "Another limitation of the current dataset concerns the emissivity. We assume snow is a perfect black-body and do not attempt to apply an emissivity model due to the lack of consensus on the topic. However, snow emissivity is known to be slightly lower than 1 (Hori et al. 2014) and to decrease with the observation angle, especially for angles over 45° in the 12-14 μm TIR window (Dozier and Warren, 1982, Hori et al., 2006). We assume this error is included in the global error, assessed by the comparison with the ground truth. To facilitate further analysis by the data users, a map of the observation angles of the area, computed as in Castel et al. (2001), is included in the dataset. Moreover, downwelling longwave measurements performed at the Col du Lautaret site are supplied (FluxAlp measurements for winter 2021-2022, AWS-North and AWS-South measurements for spring 2023). With these measurements, the surface radiative temperatures can be adjusted to accommodate emissivity values < 1".

We would also like to specify that the cold aura visible in Fig. 5 of the study is not caused by any of the three effects described above. Indeed, the black body used for the calibration - Landcal P80P has a diameter 50 mm and is located at the end of a 50 mm wide, 160 mm long cavity. It was therefore not possible to approach the TIR camera close enough to the black body source in order for it to cover the whole field of view. We therefore estimate that the gradually changing temperature at the periphery of Fig. 5 represents the cavity temperature, gradually varying towards the ambient temperature to which the casing of the black body source is exposed. In order to make this clearer in the manuscript we suggest the following addition at L189: "The Landcal P80P black-body source has a diameter 50 mm and is located at the end of a 50 mm wide and 160 mm long cavity. It was therefore not possible to approach the TIR camera close enough to the black body source to match the field of view and the area of homogeneous temperature. The calibration assessment was thus carried out using the central 240x210 pixel rectangle shown in Fig. 5." The caption of Fig. 5 was also changed accordingly.

Viewing Distance: The secondary issue is distance to sensor (Minkina & Klecha, 2016). Microbolometers are impacted by distance to the target for a number of reasons, and this also varies somewhat depending on atmospheric conditions at the time of imaging. When images are collected from a nadir position (e.g. drone/plane) this variability is minimal as height above ground can be kept relatively similar/constant (except with very complex topography). With oblique imagery this is not the case unless the target of interest is confined to a single location/distance to sensor. The manuscript presents data that is spread horizontally across 1.2km of ground from the sensor/camera to the area beyond the AWS (but excluding the very distant mountains). There is likely a significant trend in the dataset because of this. The more accurate sensors on the AWS are all located at a roughly similar distance from the camera (700m) and therefore are unlikely to pick up this effect/trend. To coarsely remedy this the authors could work out their sensors distance to target sensitivity in a lab by collecting images of a stable black body calibration plate from known distances (though extrapolating measurements from a few metres in the lab to many km in the field may be dubious and). Some cameras also provide this information within their software as a distance to target correction factor. The correction factor could then be applied to all the pixels dependent on their distance from the camera. This approach would ignore the impact of variations in atmospheric conditions between scenes and across the 1.2km distance, however this is likely much too hard to correct for.

As pointed out by [Minkina and Klecha(2016)], the measured temperature is influenced by the radiative contribution of the air between the sensor and the target. However, we did not account for this effect and consider it part of the measurement error when comparing with the ground truth at the two AWS that are much less affected by this issue. This assumption is based on the fact that the camera spectral range (8-14 µm) corresponds to the infrared atmospheric window where there is little absorption by atmospheric gases. We assess this assumption using a case during the melt season where we expect that the snow surface temperature should be homogeneous at 0°C across the landscape. In Fig. 1 we plot the surface temperature retrieved from the camera dataset along a transect (on the left) against the surface to the camera distance (on the right). We find that there is no trend (within our target uncertainty of ± 0.67K) which corroborates our assumption that the atmosphere opacity is negligible in this case (T_{air}=4.6°C, RH=57% at AWS-South). However, this assumption may not hold at times of higher air absolute humidity. Therefore, we agree with the reviewer that it is important to inform potential users about the potentially increasing error with the viewing distance due to atmospheric effects. For this, we add a distance-to-camera map to the dataset, that can be used with temperature and humidity measurements from the AWS to assess and potentially correct for the atmospheric contribution. Moreover, we add the following sentences to the manuscript:

1. In the Processing section, L216: "Our method does not include corrections for non-instrumental effects such as emissivity and atmospheric contributions. We therefore consider these effects to be included in our error estimations".

2. In the Discussion, L355: "Similarly, the measured temperature depends on the radiative contribution of the air between the sensor and the target, that was not corrected and is therefore considered part of the error measured in the comparison with the ground truth at the two AWS. Still, as this error increases with the viewing distance, a distance-to-camera map is included in the dataset, and can be used with temperature and humidity measurements from the AWS to correct for the atmospheric contribution".
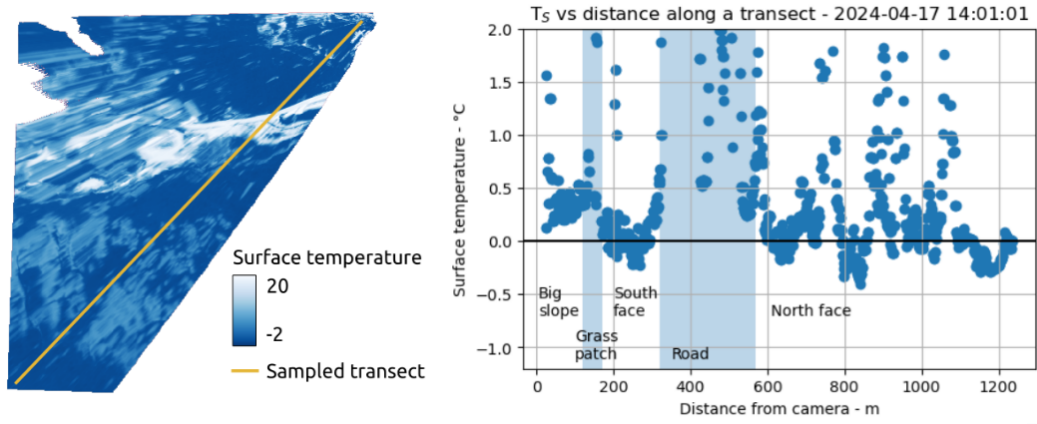
Figure 1: Snow-covered transect (on the left, yellow line) on the surface temperature map acquired on the 17-04-2024 at 14:01:01, and the measured temperature as a function of distance from the TIR camera (on the right).

Minor Comments

- AWS coordinates are provided in the readme of the datafile in decimal degrees to 4 decimal places. This means 10-13m precision (latitude dependent). Given that the TIR map product is at 2m spatial resolution, it would be better to have the AWS coordinates to 5 or 6 decimal places (1 m to 0.1 m precision) so that the field of view of the AWS IR sensors can be matched to the correct pixel within the scene. Ideally the actual centre point of what the IR sensor is looking at should also be provided as a coordinate in the readme file, not just the AWS/tower coordinates which I think are what is currently provided. ✓

- It would be useful for users to also have a georectified version of the RGB imagery made available so that users can directly link thermal maps to ground surface conditions at the pixel scale, but this is not 100% necessary and is likely to require more effort to produce.
  We agree that an orthorectified version of the RGB images could enhance the comprehension of the TIR imagery. However, the camera is still installed on the field, which made it impossible to test it for distortion parameters. As a result, our attempts to orthorectify the RGB images have not been successful.

- Line 1: temperature of 'the' snow cover – delete 'the' ✓

- Line 26: improve – change to improving? ✓

- Line 56: cal/val change to calibration-validation as used elsewhere in the manuscript. ✓

- Line 111 'in a small volume'. Here and in later sentences I think the word volume is referring to the secondary external case that the camera was placed inside (and then temperature regulated). Change volume to case/box/enclosure or something to that effect for clarity. ✓

- Line 120/121: does this refer to the temperature setting of the volume/enclosure itself? How does raising the internal temperature by 7°C (15 raised to 22C) reduce overheating? Surely that would increase overheating? Check and revise if required.
  Line 120/121 do refer to the temperature setting of the enclosure including the TIR camera. Indeed, the TEM cools off the small enclosure within the camera's casing by warming the back of the casing, where heat is expelled towards the outside through radiators installed in contact with its conductive, metallic walls. However, heat evacuation in this setup is limited and, if the external temperature is significantly higher than the TEM setting temperature, heat evacuation from the rear of the casing might become impossible. If this happens, the TEM would cause further overheating while trying to cool down the camera. Reducing the difference between the internal and external temperature - by raising the TEM setting temperature from 15°C to 22°C - reduces overheating episodes because it reduces the required heat evacuation. To make

3

this clearer in the manuscript, we modify the paragraph at L120/121 as follows: "The internal temperature of the camera was initially set to 15°C. However, this temperature proved to be too low with respect to the limited heat evacuation in the rear of the casing of this setup, causing significant overheating when the external temperature approaches 15°C. It was then raised to 22°C on the 2023-02-17 after several episodes of overheating occurred during the first week of measurements. By raising the TEM setting temperature from 15°C to 22°C, the required heat evacuation was reduced and no overheating episodes happened during the rest of the season".

- Line 141: A map showing the GCP locations could be useful, to assess the distribution and likely accuracy of this – some details on the accuracy of the georectification would also be beneficial here. I presume the GCPs were located in areas that were not snow covered during the winter and are constant and visible in every image? Also providing these GCP coordinates so that others can orthorectify the RGB imagery if it is not to be provided in a map format would be useful. I'm also wondering how well the 100x70cm GCPs were visible in the TIR imagery which is provided at a 2m spatial resolution. If the GCPs are well distributed across the survey area and can be assumed to accurately reflect sky temperature only (i.e. constant and stable for a given image) then perhaps they could be useful for identifying potential errors in Ts resulting from view angle and distance to target.
  A table containing the list of GCPs and the projection error computed by the Ames Stereo Pipeline software for the years 2022 and 2023 was added to the manuscript in the Appendix A. The following sentences are added to the manuscript:

  - L145: "Their positions both in world and camera coordinates are listed in Table A1 and Table A2 and shown in Fig. A1 and Fig. A2 in Appendix A."
  - L300: "The projection error for each GCPs is listed in Table A1 and Table A2 in Appendix A."

  The GCPs' positions were indeed acquired during the winter season for both years, with snow covering the ground. To compensate for the presence of the snow cover, 0.75 m were added to the DEM used for the orthoprojection. According to the distance from the TIR camera, the aluminum plate used to extract the GCPs position is identified as a 1 to 2 pixel cold spot appearing at the time of acquisition. However, because of its small size, the aluminum plate is not completely resolved in the image and we cannot use its temperature as a measurement for the sky temperature.

- Table 2: lat long are presented to 6 sig fig precision (5dp longitude, 4dp latitude). These should be at least 5dp precision (ideally 6dp) in all cases so we are at metre scale accuracy at minimum. ✓

- Figure 11: a density scatterplot might better show the distribution of this many points. I think the black line is the 0/0 line and not the R2 linear fit? Please add linear fit along with R2 and RMSE. From the 2023 figure it looks like there is a warm bias in the camera measurement that increases with surface temperature (excluding the section circled in red), it might be worth discussing this too.
  As suggested, Figure 11 was replaced by two density scatterplots. The linear regressions were computed and the slope, intercept, RMSE and R^2 of each are listed. The caption is modified as: "Density distributions of the snow surface temperatures measured at AWS-South by the camera as a function of those measured by the radiometer during winter 2021-2022 (a), and spring 2023 (b). The plot shows the high measurements of the surface temperature measured during spring 2023 over melting snow (red circle). Also shown are the identity line (dotted gray) and the linear regression of the distributions (orange)." Moreover, the following paragraph is added to the end of the Validation section: "Also illustrated in Fig. 11 are the linear regressions of the two distributions (orange lines), the computed slopes, intercepts, fit R^2 and RMSE (respectively m, b, R^2 and σ_y). Both distributions confidently fit to the regression, as shown by the elevated R^2, 0.96 for winter 2021-2022, 0.97 for spring 2023. The first has an intercept b=-1.81°C with the error decreasing with the temperature as the slope m=0.91. The second, on the other hand, has an intercept b=+0.52°C and the bias is fairly constant as m=1.02."

- Line 346 – I have also noticed this warm temp in my own work of TIR imaging of melting snow/ice where I would expect 0°C. I wonder if it could be due to the camera actually measuring the temperature of a thin film of melt water sitting atop the snow/ice which could potentially exceed the 0°C of the snow/ice surface proper?
  We have evaluated this hypothesis. Assuming a thermal conductivity of water k=0.6 and a water film thickness of 0.5 mm, 1200 Wm^{-2} of absorbed energy would be needed to sustain a 1 K difference between the top layer and the bottom snow layer at 0°C, which is not plausible. In order to clarify this aspect, we modify L346 as follows: "We tested the possibility that the higher error for melting snow might be due to a thin layer of warmer water above the snow grains. However, assuming a thermal conductivity of water k=0.6 and a water film thickness of 0.5 mm, 1200 Wm^{-2} of absorbed energy would be needed to sustain a 1 K difference between the top layer and the bottom snow layer at 0°C, which is not plausible. Therefore, the physical cause of this error is unidentified and remains to investigate."

Finally, although not requested by the reviewers, two figures were added to the manuscript to highlight the utility of the dataset. The first is a full timeseries of the snow surface temperature measured at AWS-South from between December 2022 and May 2023, compared with the TIR radiometer. The second illustrates four examples of spatial patterns of the snow surface temperature under different atmospheric conditions: a night with clear sky, a day with clear sky, a cloudy day and a melting day. To implement these figures, L376 was modified as follows: "The full timeseries are shown in Fig. 13. Finally, the images in Fig. 14, acquired under different atmospheric conditions, show the variability of the patterns of the surface temperature of snow caught by the TIR camera. Beside these examples, the dataset provides numerous other situations that deserve further exploration."

References

[Litwa(2010)] Litwa, M.: Influence of angle of view on temperature measurements using thermovision camera, IEEE Sensors Journal, 10, 1552–1554, https://doi.org/10.1109/JSEN.2010.2045651, 2010.

[Minkina and Klecha(2016)] Minkina, W. and Klecha, D.: Atmospheric transmission coefficient modelling in the infrared for thermovision measurements, Journal of Sensors and Sensor Systems, 5, 17–23, https://doi.org/10.5194/jsss-5-17-2016, 2016.